Osmotically Activated Agent Release From Electrostatically Generated Polymer Microbeads

Brian G. Amsden
Dept. of Chemical Engineering, Queen's University, Kingston, Ontario, Canada K7L 3N6

Release of lysozyme from poly(ethylene-co-vinyl acetate) microbeads into solution was examined. The lysozyme exists as solid particles dispersed randomly throughout the polymer matrix. Microbeads were prepared in a novel fashion using electrostatics to reduce bead sizes, which ranged from 0.6−0.43 to 1.0−0.85 mm. The release into distilled water was diffusionally controlled, followed by a period of osmotically controlled transport, which lasted for up to 400 hours for 1.0−0.85-mm microbeads. The osmotically controlled release rate increased as the microbead radius increased, and was time- and weakly particle-size-dependent, decreasing with time and being initially greater for larger particles, but eventually becoming greater for smaller particles as time progressed. For example, for 0.60−0.43-mm microbeads, the initial mass fraction release rate from microbeads containing 106−75-μm particles was 0.0074 h^{-1}, while that of microbeads containing $\leq$ 53-μm particles was 0.0068 h^{-1}. At 100 h, however, the release rate from microbeads containing 106−75-μm particles was 0.0024 h^{-1}, while that of microbeads containing $\leq$ 53-μm particles was 0.0029 h^{-1}. The total fraction of agent released from the polymer matrix increased, as the agent particle size increased and as the microbead radius decreased. A mathematical model of the osmotic release mechanism developed was consistent with the experimental observations. This model can be used in the design of controlled release products for pharmaceutical, agricultural and veterinarial applications.

Introduction

Controlled release products provide prolonged delivery of an agent at a predetermined, predictable rate. There are a number of advantages associated with these products, particularly in the field of pharmaceutics. These advantages include utilizing the drug more efficiently by delivering it directly to the target tissue thereby reducing potential side effects, reducing the number of required applications, and maintaining the drug within its therapeutic range. As a result, controlled release improves patient comfort and compliance. A further incentive for the development of controlled release products is their economic value. Companies that develop new drugs eventually lose market share to generic drug manufacturers once the patents for the drugs expire. A means of combating this competition, and to extend patent protection, is to provide longer dosage schedules and safer delivery profiles through controlled release technologies.

Polymeric matrix systems have been investigated for use in controlled drug delivery because of the relatively benign and simple nature of the fabrication procedure. Other advantages of these drug delivery systems are that they prevent drug degradation prior to its release by prohibiting contact with the external solution until release occurs, and dose dumping of the drug should the device fail. In these devices the drug is dispersed as solid particles within a biocompatible polymer. Release of the drug is typically time-dependent, indicating diffusional transport control. An often desirable feature of a controlled release device, however, is the ability to sustain a constant release rate (Baker, 1987). Substantial progress has been made over the past two decades in the development of delivery devices that provide such a delivery rate. One such strategy uses osmotic pressure as the driving force (Gale et al., 1980; Carelli et al., 1989; Amsden and Cheng, 1995).

Agent release from these systems begins with the dissolution and subsequent diffusion of those particles in intimate contact with each other and the device surface. The amount

Current address of B. G. Amsden: Angiotech Pharmaceuticals Inc., Box 4, 303-2386 East Mall, UBC, Vancouver BC, Canada V6T 1Z3.

of the initially loaded agent released in this manner is dictated by the initial volume loading of the agent in the polymer-agent matrix and has been described in terms of a modified percolation theory (Saltzman and Langer, 1989; Siegel et al., 1989). At low loadings, only a small fraction of the agent can be released. Above a critical loading fraction, most of the agent particles are intimately connected to form a percolating cluster, or in other words, a wholly interconnected porous network throughout the matrix which reaches a surface. The quantity of agent released thus increases dramatically, and agent release from the matrix is diffusionally controlled. Osmotically controlled release has been shown to dominate for situations wherein the agent is loaded at volume fractions below the critical fraction if the agent is sufficiently osmotic (Gale et al., 1980; Amsden et al., 1994).

Osmotically activated release of agents from a polymer matrix device has been studied for a number of years (Marson, 1969; Fossey and Smith, 1973; Narkis and Narkis, 1976; McGinity et al., 1979; Fedors, 1980; Gale et al., 1980; Wright et al., 1981; Di Colo et al., 1984; Carelli et al., 1989; Schirrer et al., 1992; Zhang et al., 1993; Amsden and Cheng, 1994). The type of release kinetics observed depends on the properties of the polymer used. With brittle polymers, the release rates are Fickian in nature (Marson, 1969; Narkis and Narkis, 1976; Zhang et al., 1993). Osmotically driven agent release from rubbery materials is characterized by a period of pseudo-constant release attained after an initial burst of agent (Gale et al., 1980; Di Colo et al., 1984; Carelli et al., 1989; Schirrer et al., 1992) and a total fraction of agent released greater than that predicted by percolation effects (Amsden and Cheng, 1994). This discussion is concerned only with release from rubbery or elastomeric materials.

The following mechanism has emerged (Figure 1). Upon immersion of the polymer-agent matrix into an aqueous solution, those particles exposed at the surface, and any in intimate contact with them, dissolve and diffuse away from the surface resulting in an initial burst of material from the device. At the same time, water vapor diffuses slowly through the polymer until it reaches a polymer encapsulated particle, hereafter called a capsule. The water phase-separates and dissolves the agent at the capsule/polymer interface to eventually create a saturated agent solution, thereby producing a greater activity gradient between the capsule and the surrounding aqueous solution. Under this activity gradient, water is drawn more rapidly into the capsule increasing its internal pressure.

This pressure, the osmotic pressure of the solution, acts radially outwards and deforms the surrounding elastomeric polymer wall reducing the wall thickness. The polymer in turn exerts a resisting pressure on the expanding capsule. Water continues to be drawn into the capsule until a critical wall thickness is reached or until an equilibrium is established between the internal pressure of the capsule and the resisting pressure of the polymer (Schirrer et al., 1992; Amsden and Cheng, 1994). In the latter case, no material is released. If the capsule wall thickness reaches a critical limit, the wall will break creating fissures in the polymer. These fissures form a percolating cluster through which the agent is released. The polymer then relaxes back to its original state. The relaxation process forces saturated agent solution from the capsule and into the pore network. This solution displaces an equal volume of solution in the pores near the device surface. The process repeats in a serial fashion towards the center of the device as each cross-sectional layer of capsules ruptures.

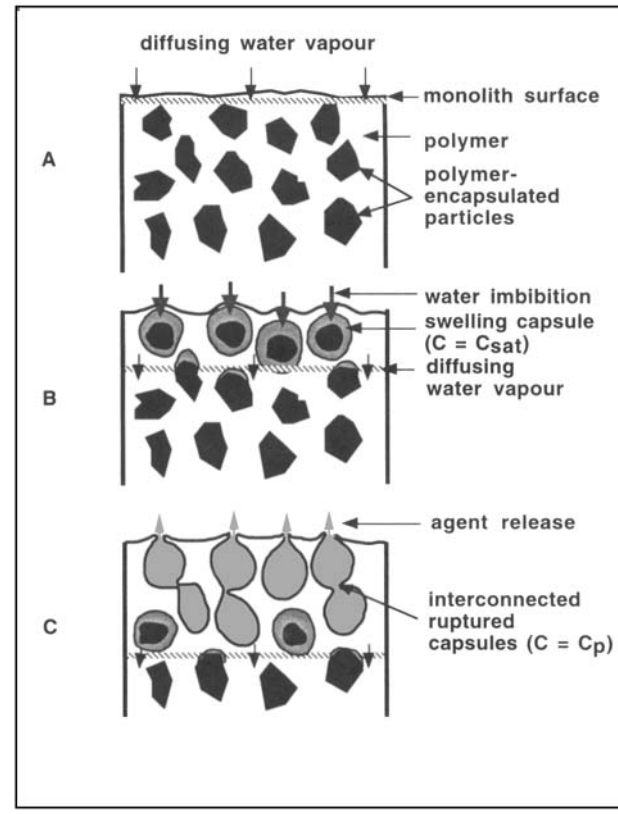

Figure 1. Proposed osmotic release mechanism.

(a) Water diffusion through polymer to first layer of agent particles; (b) swelling of particle capsules due to water imbibition under an osmotic activity gradient; (c) interconnected pore network formation and agent release as a result of capsule rupturing.

As the term controlled release implies, it is important to be able to determine and regulate the release rate from the device. For this reason, mathematical models have been developed to determine factors affecting both the release rate (Wright et al., 1981; Schirrer et al., 1992; Amsden et al., 1994) and the total fraction released (Amsden and Cheng, 1994). In each of the models describing the release rate, it is assumed that the time required to rupture the capsule is the dominant time factor. Common weaknesses of both the model of Wright et al. and that of Schirrer et al. are: (1) assuming that the water influx per unit time and unit area during the capsule swelling phase is constant; (2) neglecting to account for the resisting pressure of the polymer when determining the time required to rupture a capsule; and (3) assuming that all the capsules rupture. Recently, these limitations have been removed in the development of a model to explain the release behavior from a polymer-agent matrix slab (Amsden et al., 1994).

As the desired device geometry is not always rectangular, the concepts employed in developing the slab model were extended in this article to spherical matrices. The model derived was used to explain the release profiles of a protein drug analog, lysozyme, from poly(ethylene-co-vinyl acetate) microbeads. The protein-loaded microbeads were prepared

in a novel fashion by utilizing electrostatics. The model should prove useful in the design of controlled release products for pharmaceutical, agricultural, and veterinarial applications.

Model Development

In the succeeding model development the following simplifying assumptions are made:

(1) The polymer is an incompressible (i.e., it has a Poisson ratio approximately = 0.5), isotropic, Hookean material.

(2) The agent particles are uniform in size, homogeneously distributed, and spherical.

(3) The agent capsules swell spherically in an isotropic fashion.

(4) The osmotic pressure during the swelling phase up to the point of rupture is constant and equal to the osmotic pressure of a saturated agent solution.

(5) Capsule swelling and rupturing proceeds in a serial manner through the device from the surface to the center. In other words, the capsules in the cross-sectional layer closest to the surface rupture before any in the next layer rupture.

The mass of agent released by osmotic pressure induced polymer rupturing m with time t can be expressed as (Wright et al., 1981)

$$\frac{dm}{dt} = \frac{M_L}{t_b + t_p} \tag{1}$$

in which M_L is the mass of agent released per cross-sectional layer of the device, t_b is the time required to rupture a capsule, and t_p is the time during which solution is forced from the ruptured capsule. M_L is defined as,

$$M_L = n_b V_b C_p \tag{2}$$

where C_p is solute concentration in the pores near the surface, V_b is the volume of water drawn into the capsule at the point of rupture, and n_b is the number of ruptured capsules per layer.

The number of ruptured capsules per layer is determined by recognizing that not all capsules within the matrix will rupture. The total mass fraction of agent released from the matrix Q can be divided into two components, the mass fraction released by dissolution and diffusion Q_D, and the mass fraction released by osmotic pressure induced capsule rupturing Q_Π (Amsden and Cheng, 1994). The agent particles are distributed randomly throughout the matrix and thus there is a distribution of distances between particles. These distances can be considered to be capsule wall thicknesses h whose distribution throughout the matrix can be represented by the function $f(h)$. Only those capsules with initial (i.e., before swelling) wall thicknesses less than a critical wall thickness h_c will rupture. The fraction of encapsulated particles within the matrix is given by $(1 - Q_D)$. The fraction of the capsules that rupture θ is therefore

$$\theta = \frac{Q_\Pi}{1 - Q_D} \tag{3}$$

or in terms of $f(h)$,

$$\theta = \int_0^{h_c} f(h)\,dh \tag{4}$$

Equation 4 allows for the determination of θ without having to perform experiments if the distribution can be estimated. It has been demonstrated that a Weibull distribution function can be used (Amsden and Cheng, 1994). Using this distribution function and integrating Eq. 4 gives

$$\theta = 1 - \exp\left[-\frac{\pi}{4}\left(\frac{h_c}{\bar{h}}\right)^2\right] \tag{5}$$

where $\bar{h}$ is the average distance between encapsulated particles before release.

The average distance between encapsulated particles within the microbead was estimated by assuming an ideal situation in which the particles were distributed equidistantly within a cube of volume equal to the volume of the microbead. Assuming further that none of the particles are exposed at a surface, $\bar{h}$ is given by

$$\bar{h} = \frac{L - nd}{n + 1} \tag{6}$$

in which n is the number of spherical particles in any one-dimensional direction within the cube, d is the diameter of a cube of equal volume as the spherical particle, and L is the length of the cubic matrix. From geometric considerations, n is given by

$$n = \frac{L}{d}\phi^{1/3} \tag{7}$$

where ϕ is the volume fraction of agent within the matrix. Substituting for n results in

$$\bar{h} = \frac{dL(1 - \phi^{1/3})}{L\phi^{1/3} + 1} \tag{8}$$

Using the definitions for L and d, Eq. 8 becomes

$$\bar{h} = \frac{\left(\frac{4\pi}{3}\right)^{1/3} r_o R[1 - \phi^{1/3}]}{R\phi^{1/3} + r_o} \tag{9}$$

where R is the bead radius and r_o is the radius of the particle.

It remains to estimate the critical wall thickness h_c which is related to the wall thickness of the swelling capsule at the point at which it ruptures. If it is assumed that the capsule is spherical, a force balance around the swelling particle can be used to determine the wall thickness at rupture h_r (Figure 2). The force of the osmotic pressure $\Delta\Pi$ acting so as to lift the top half of the capsule $\Delta\Pi(\pi r^2)$ is balanced by the tensile stress σ acting over the capsule wall cross-sectional area $\pi[(r + h)^2 - r^2]$. At the point at which the capsule is just about to rupture

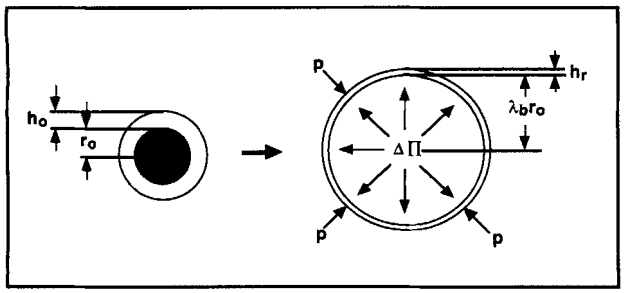

Figure 2. Swelling capsule showing capsule dimensions, the osmotic pressure $\Delta\Pi$ acting to expand the capsule, and the resisting polymer pressure p.

Capsule on the left depicts an encapsulated particle within the matrix before water imbibition, while capsule on the right depicts a water-swollen capsule about to rupture.

$$h_r = r\left(\sqrt{1+\frac{\Delta\Pi}{\sigma_b}}-1\right) \tag{10}$$

wherein r is the radius of the capsule at rupture, and σ_b is the tensile strength of the polymer at rupture. The volume of the capsule wall remains constant while it swells, therefore

$$(r_o+h_c)^3 - r_o^3 = (r+h_r)^3 - r^3 \tag{11a}$$

By defining $r = r_o\lambda_b$, where λ_b is the radial extension ratio of the capsule at rupture, and substituting this in Eq. 8, Eq. 9 can be expressed as

$$\beta^3+3\beta^2+3\beta = \lambda_b^3(3\gamma+3\gamma^2+\gamma^3)$$

in which β (dimensionless constant) $= h_c/r_o$ and $\gamma = \sqrt{1+\Delta\Pi/(\sigma_b)}-1$ (γ is a dimensionless constant). Solving for β yields

$$\beta = [1+\lambda_b^3(\gamma^3+3\gamma^2+3\gamma)]^{1/3}-1 \tag{11b}$$

The fraction of capsules that rupture is therefore

$$\theta = 1-\exp\left[-\frac{\pi}{4}\left(\frac{\beta(R\phi^{1/3}+r_o)}{\left(\frac{4\pi}{3}\right)^{1/3}R[1-\phi^{1/3}]}\right)^2\right] \tag{12}$$

Equation 12 represents a theoretical improvement in the prediction of θ over a previous model (Amsden and Cheng, 1994) in that it can account for the experimentally observed increase in θ with increased particle size r_o.

The total number of capsules that rupture per microbead N can now be expressed as

$$N = \theta(1-Q_D)\phi\left(\frac{R}{r_o}\right)^3 \tag{13}$$

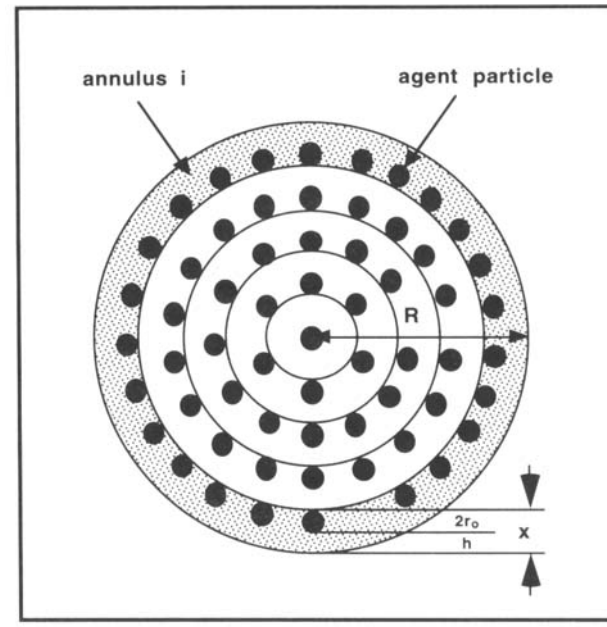

Figure 3. Agent-loaded microbead as a concentrically layered sphere showing the microbead radius R, the particle radius r_o, the capsule wall thickness h, and the annulus thickness x.

To determine n_b, the microbead is pictured as being composed of concentric annuli, much like the layers of an onion (Figure 3). The number of beads per layer is equal to N times the volume of the annulus defining that layer divided by the total volume of the microbead. The thickness of each annulus x is assumed to be constant and equal to $(\bar{h}+2r_o)$. The volume of the annulus in question at time t is thereby

$$V_i = \frac{4\pi}{3}[(R-(i-1)x)^3-(R-ix)^3] \tag{14}$$

wherein i represents the annulus which is in the process of being ruptured at time t. This annulus can be defined as t/t_b. Expanding Eq. 14, dividing by the volume of the microbead and substituting for N yields

$$n_b = \theta(1-Q_D)\phi\left(\frac{R}{r_o}\right)^3\left[a-b\left(\frac{t}{t_b}\right)+c\left(\frac{t}{t_b}\right)^2\right] \tag{15}$$

where

$$a = 3\frac{x}{R}+3\left(\frac{x}{R}\right)^2+\left(\frac{x}{R}\right)^3 \tag{16}$$

$$b = 6\left(\frac{x}{R}\right)^2+3\left(\frac{x}{R}\right)^3 \tag{17}$$

$$c = 3\left(\frac{x}{R}\right)^3 \tag{18}$$

Thus, as the rupturing front moves towards the microbead center, the number of particles that are released decreases. (a, b, and c are dimensionless geometric constants.)

To complete the definition of M_L, the volume of water which has been imbibed once the capsule ruptures is defined as

$$V_b = \frac{4\pi}{3} r_o^3 (\lambda_b^3 - 1) \tag{19}$$

and C_p is defined as (Amsden et al., 1994)

$$C_p = \exp\left(- \frac{DA_o t_b}{V_f h} \right) C_s = \omega C_s \tag{20}$$

where D is the agent diffusivity, A_o is the area of the opening created by the rupturing of the capsule wall, and V_f is the volume of the capsule after it ruptures and the agent saturated solution has been forced out.

Previously, it has been shown that t_b is much greater than t_p (Amsden et al., 1994). Therefore, t_p can be ignored and the mass of agent released from the microbead during the osmotic bursting phase can be solved by substituting Eqs. 15, 19 and 20 into Eq. 2 and integrating.

$$m = \theta(1 - Q_D)\omega C_s(\lambda_b^3 - 1)\phi \frac{4\pi}{3} R^3 \left[a\left(\frac{t}{t_b}\right) - \frac{b}{2}\left(\frac{t}{t_b}\right)^2 + \frac{c}{3}\left(\frac{t}{t_b}\right)^3 \right] \tag{21}$$

The release rate can also be expressed in terms of the fraction of the initially loaded agent released by noting that the initial mass of agent in the microbead m_i is,

$$m_i = \rho\phi \frac{4\pi}{3} R^3 \tag{22}$$

where ρ is the density of the agent. Thus, the osmotic mass fraction released at time t ($Q_{\Pi,t}$) is given by

$$Q_{\Pi,t} = \frac{\theta(1 - Q_D)\omega C_s(\lambda_b^3 - 1)}{\rho} \left[a\left(\frac{t}{t_b}\right) - \frac{b}{2}\left(\frac{t}{t_b}\right)^2 + \frac{c}{3}\left(\frac{t}{t_b}\right)^3 \right] \tag{23}$$

The value of ω (dimensionless constant) can be estimated by recognizing that once the final layer of capsules ruptures (i.e., when $t/t_b = R/x$) $Q_{\Pi,t} \le \theta(1 - Q_D)$ and therefore

$$\omega \le \frac{\rho}{C_s(\lambda_b^3 - 1)\left[a\left(\frac{R}{x}\right) - \frac{b}{2}\left(\frac{R}{x}\right)^2 + \frac{c}{3}\left(\frac{R}{x}\right)^3 \right]} \tag{24}$$

Using Eq. 24 for ω results in the following expression for the mass fraction of drug released

$$Q_{\Pi,t} = \frac{\theta(1 - Q_D)}{\left[a\left(\frac{R}{x}\right) - \frac{b}{2}\left(\frac{R}{x}\right)^2 + \frac{c}{3}\left(\frac{R}{x}\right)^3 \right]} \times \left[a\left(\frac{t}{t_b}\right) - \frac{b}{2}\left(\frac{t}{t_b}\right)^2 + \frac{c}{3}\left(\frac{t}{t_b}\right)^3 \right] \tag{25}$$

Determination of time required to rupture capsule

The time required to rupture a capsule t_b can be estimated by considering a single capsule (Kuethe et al., 1992). The time to rupture the capsule is governed by the rate at which the capsule swells which in turn depends on the rate at which the capsule draws in water. Water imbibition into a capsule is given by

$$\frac{dV}{dt} = \frac{kA_i}{h}(\Delta\Pi - p) \tag{26}$$

wherein V is the volume of water imbibed, k is the osmotic permeability of the polymer, A_i is the capsule membrane area for imbibition, and p is the resisting pressure of the polymer.

Equation 26 can be expressed in terms of the capsule radius r as,

$$\frac{dr}{dt} = \frac{k(r + h)^2}{r^2 h}(\Delta\Pi - p) \tag{27}$$

As the capsule swells, the thickness of the membrane will decrease. The assumption of an incompressible material requires that the membrane volume remains constant during swelling. The capsule wall thickness h can therefore be expressed in terms of r as follows

$$(h + r)^3 - r^3 = (h_o + r_o)^3 - r_o^3 \tag{28}$$

in which h_o is the median wall thickness of those capsules within the microbead that do rupture. h_o can be estimated from

$$0.5 = \frac{1 - \exp\left[- \frac{\pi}{4}\left(\frac{h_o}{\bar{h}}\right)^2 \right]}{\theta} \tag{29}$$

Rearranging Eq. 29 yields

$$h_o = \frac{2r_o L(1 - \phi^{1/3})}{L\phi^{1/3} + 1} \sqrt{ - \frac{4}{\pi} \ln\left(1 - \frac{\theta}{2}\right)} = \chi r_o \tag{30}$$

Substituting Eq. 30 into Eq. 28 and solving for h gives

$$h = (r^3 + \xi r_o^3)^{1/3} - r \tag{31}$$

where

$$\xi = (\chi + 1)^3 - 1 \tag{32}$$

(χ and ξ are dimensionless constants.) Finally, it is necessary to calculate the resisting pressure of the polymer. Using a force balance around the swelling capsule, as was done to determine the wall thickness at rupture, yields,

$$p = \frac{\sigma(h^2 + 2hr)}{r^2} \tag{33}$$

where σ is the tensile stress of the polymer. By assuming that the polymer behaves as a Hookean material, tensile stress can be written as

$$\sigma = E\frac{(r - r_o)}{r_o} \tag{34}$$

in which E is the Young's modulus of the polymer. Therefore, the resisting pressure of the polymer is given by

$$p = \frac{E(r - r_o)}{r_o}\frac{(h^2 + 2hr)}{r^2} \tag{35}$$

Now Eq. 27 can be written as

$$\frac{dr}{dt} = \frac{k(r+h)^2}{r^2 h}\left[\Delta\Pi - \frac{E(r - r_o)}{r_o}\frac{(h^2 + 2hr)}{r^2}\right] \tag{36}$$

Expressing Eq. 36 in terms of the radial extension coefficient $\lambda = r/r_o$ results in

$$\frac{d\lambda}{dt} = \frac{k}{r_o^2}\frac{(\lambda + h^*)^2}{\lambda^2 h^*}\left[\Delta\Pi - \frac{E(\lambda - 1)(h^{*2} + 2h^*\lambda)}{\lambda^2}\right] \tag{37}$$

where

$$h^* = (\lambda^3 + \xi)^{1/3} - \lambda \tag{38}$$

The time required to rupture the capsule is then

$$t_b = \frac{r_o^2}{k}\int_1^{\lambda_b} \frac{\lambda^4 h^*}{(\lambda + h^*)^2[\Delta\Pi - E(\lambda - 1)(h^{*2} + 2h^*\lambda)]}\, d\lambda \tag{39}$$

Equation 39 must be integrated numerically. (h^* is dimensionless wall thickness.)

According to the derived model, for $x \ll R$ and during the initial phase of osmotic release, the first term in the polynomial expression of Eq. 25 dominates and there will be a brief period of approximately constant release. The release rate will then decrease with time, even though the osmotic rupturing mechanism dominates. This decline is a result of the reduced number of capsules per layer available as the zone of ruptured capsules moves towards the center of the bead. The same effect would be realized for a cylindrical device which releases agent radially, a fact not accounted for by Schirrer et al. (1992). For slab geometries, in which the mass of agent released per layer can be considered to be constant, the release rate remains constant (Gale et al., 1980; Wright et al., 1981; Amsden et al., 1994).

The model has been developed to describe the situation in which agent release is predominantly osmotically controlled, which occurs at agent loadings below a critical volume fraction. Under this condition, the rate of water uptake into the pores does not limit the release rate. However, above the critical loading, where the pore network within the matrix becomes extensive, the rate at which water is drawn into the pores could limit the osmotic release rate. Nonetheless, it has been observed for the release of inorganic salts from EVA slabs loaded above the critical loading that the release rates appeared to be diffusionally controlled, but did not follow the order of the diffusion coefficients (Amsden et al., 1994). The release rates instead were greatest for the salts having the greatest osmotic pressure.

Materials and Methods

Lysozyme-HCl (LYS), bovine serum albumin (BSA), sodium chloride, and sodium azide were purchased from SIGMA, USA. Elvax-40 (poly(ethylene-covinyl acetate) (EVA) consisting of 40% vinyl acetate) was graciously donated by Du Pont, Canada. Dry protein was sieved into the following particle-size ranges (in μm): 107–75, and < 53. All other chemicals were used as received.

Microbead preparation

The method used for preparing the protein loaded EVA microbeads is a variation of the method of Sefton et al. (1984). The protein particles were suspended in a 10% EVA-dichloromethane solution. The solution was then poured into a stirred, sealed flask as illustrated in Figure 4. Air pressure was used to force the protein/dissolved EVA suspension through glass tubing and finally through a 16 gauge needle. A positive electrode was connected to the needle while a ground was applied to the collecting solution 4 cm below the needle. The collecting solution consisted of methanol cooled to -75°C using a dry ice/methanol bath contained in a dewar flask. The applied voltage was varied from 3.5 to 4.5 kV in order to obtain a wide range of microbead sizes. For a discus-

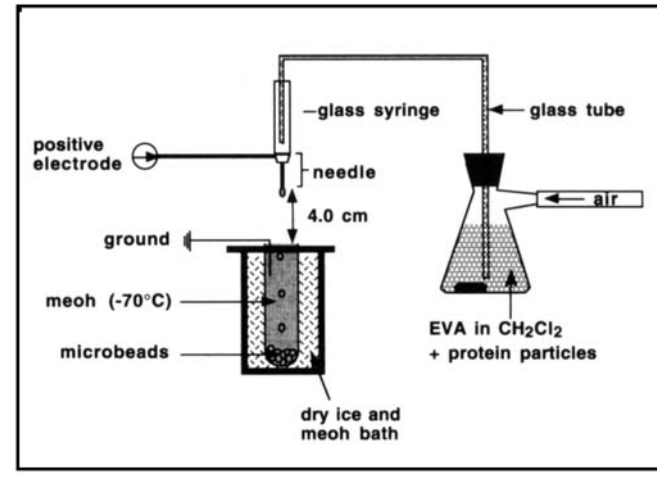

Figure 4. Electrostatic extrusion apparatus used to prepare protein loaded EVA microbeads.

sion of the mechanism of electrostatic droplet formation, refer to Bugarski et al. (1994a,b) and Amsden and Goosen (1996).

Upon entering the collecting solution, the EVA promptly precipitated. The EVA/protein microbeads were left in the cold methanol for 5 min and then transferred along with the methanol into a glass petri dish and placed in a −20°C environment for 2 days. The petri dish was then placed *in vacuo* at room temperature for one day to ensure complete solvent removal. The microbeads were sieved into the following size ranges (in mm): 1–0.85, 0.85–0.71, 0.71–0.60, and 0.60–0.43. The average bead size diameters were determined using JAVA (Jandel Scientific) image analysis software.

Release studies

Between 0.025 and 0.050 g of the microbeads were added to 20 mL of the release medium in 25 mL scintillation vials. The vials were then placed on a shaker bath maintained at 25°C and stirred at 250 rpm. At each sampling period, 1 mL of release medium was removed and replaced with fresh medium. The removed sample was analyzed for LYS via UV absorption at 280 nm. All tests were done in triplicate. The release medium was either 0.02% sodium azide in distilled water, or a saline solution of varying osmotic strength. Release into saline solution was used to determine Q_D.

Mechanical properties of EVA

The physical properties of EVA were tested by preparing the EVA sample in a manner as similar as possible to the conditions of the microbead fabrication procedure. A 10% EVA in dichloromethane solution was poured into a precooled (approximately −70°C) aluminum mold which was quickly and gently placed into a methanol bath cooled to around −70°C using dry ice. The mold was left in the methanol bath for 5 min and then transferred to a freezer kept at −20°C. After 24 h, the mold was put into a vacuum and kept under a vacuum of 25 psia at room temperature for 2 days. The sample was tested at 25°C on an Instron, as per ASTM Standard D638-64T, using a crosshead speed of 50 cm/min. Three samples were used to determine an average value for the tensile strength at rupture and the Young's modulus of EVA.

Environmental scanning electron microscope images

Photographs of the microbead surfaces were taken using an ElectroScan Model E-3 environmental scanning electron microscope (ESEM). This microscope allows samples to be viewed in their natural states at high accelerating voltages without the need for coating or other specimen preparation. An ESEM also operates at higher pressures than a conventional SEM. The microbeads were secured to a specimen stub using conductive carbon paint and viewed at a pressure of 4–5 torr with an accelerating voltage of 20 kV.

Results and Discussion

As osmotic release from matrix systems dominates at agent loadings below a critical volumetric loading ϕ_c, it was necessary to find the approximate value of this critical loading experimentally since *a priori* evaluations are not possible. Thus, BSA loaded microbeads of varying microbead radius and of two agent particle sizes were immersed in iso-osmotic saline and the total fraction released determined. The osmotic pressure of a saturated BSA solution in distilled water (pH = 6.0) has been estimated as 0.87 MPa (Amsden, 1996) by extrapolating the data of Scatchard et al. (1946) to a saturated BSA concentration of 0.59 g/mL (Saltzman and Langer, 1989). The total fraction released in this manner was considered the diffusional fraction released Q_D. ϕ_c was estimated as the volume fraction at which the cumulative mass fraction released began to increase rapidly. The critical volumetric loading was approximately 0.40 for beads made with 106–75 μm BSA particles and 0.45 for beads made with particles of < 53 μm (Figures 5a and 5b). Accordingly, experiments were done to test the osmotic rupturing model using volumetric loadings of 0.35. This volume fraction was chosen because it is below the

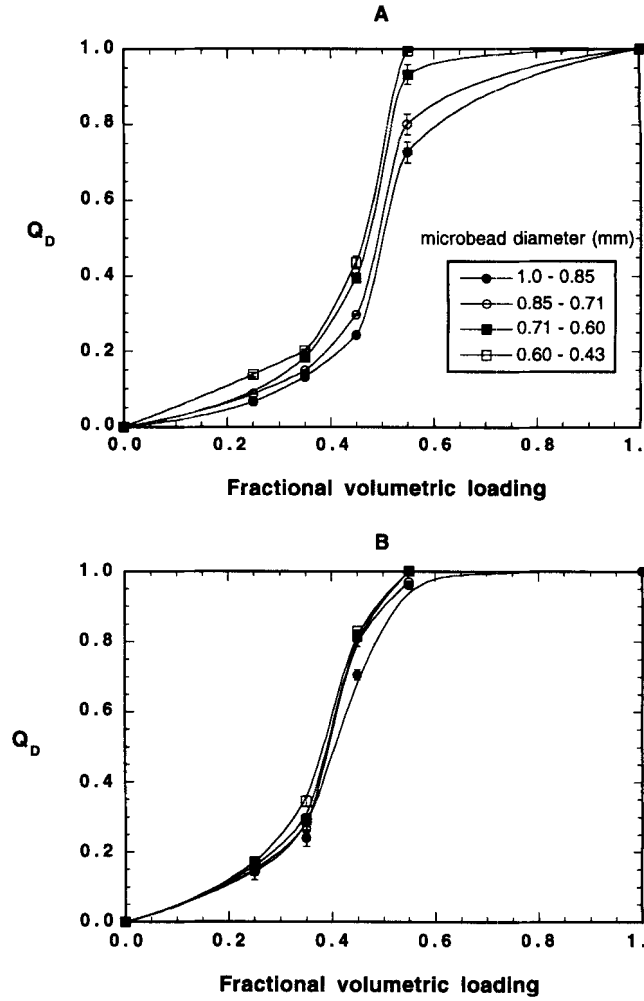

Figure 5. Total mass fraction released by diffusion vs. initial fractional volumetric loading for BSA-loaded EVA microbeads released into iso-osmotic (1.2 w/v%) saline, as a function of microbead diameter and BSA particle size.

Each point represents the average and the error bars represent the standard deviation of three samples. (a) microbeads containing < 53 μm BSA particles; (b) microbeads containing 106–75 μm BSA particles.

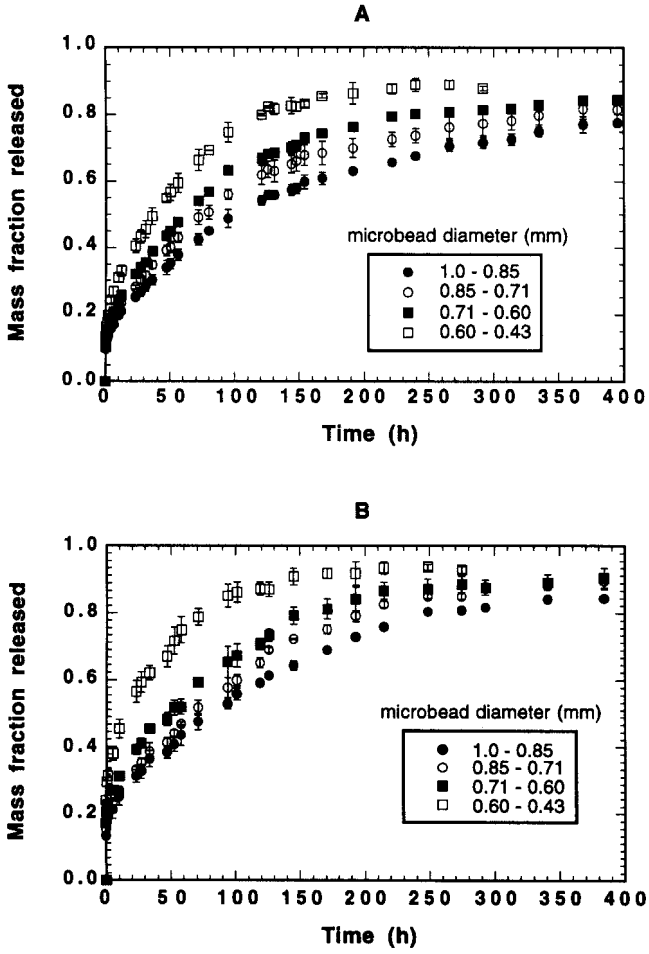

Figure 6. Mass fraction of LYS released vs. time for microbeads of varying average diameter and varying LYS particle size.

Each point represents the average and the error bars represent the standard deviation of three samples. (a) Microbeads containing < 53 μm LYS particles; (b) microbeads containing 106–75 μm LYS particles.

critical volume fraction for both particle sizes examined and because it should result in a relatively large mass fraction of protein released by the osmotic pressure mechanism, as predicted by Eq. 12.

The release profiles of the LYS loaded microbeads immersed in distilled water are displayed in Figures 6a and 6b. The figures show that the release rate increased as the microbead size decreased and as the particle size of the LYS used increased. The microbeads exhibited a prolonged release duration, reaching over 400 h. The total mass fraction of the protein released was greater than about 0.77 for all the microbeads examined, and decreased as the microbead size increased. For instance, the total mass fraction of LYS released from 1.0–0.85 mm microbeads containing < 53 μm particles was 0.78 whereas the total mass fraction released from the 0.60–0.43 mm microbeads was 0.88. It is not clear from this figure, however, whether osmotically activated release is occurring.

Osmotic pressure induced release results from polymer encapsulated particles within the protein/polymer matrix drawing in water from the external medium at a rate proportional to the water activity gradient across the polymer barrier. This influx of water increases the internal pressure of the capsule until the surrounding polymer wall ruptures, releasing the capsule protein solution. Thus, the release rate can be reduced by decreasing the water activity of the release medium. If the water activity of the release medium is equal to or less than the water activity of a saturated solution of the protein solution then osmotic release will not occur. This principle has been demonstrated by Gale et al (1980), Wright et al. (1981), and Amsden and Cheng (1994).

Table 1. Isoosmotic Saline Compositions

g/100 mL NaCl	Osmotic Pressure (MPa)*
0.26	0.20
0.58	0.45
1.17	0.87
1.94	1.50
3.22	2.51
4.09	3.17

*At 25°C from data in Robinson and Stokes (1965).

Therefore, to confirm that osmotically activated release from the microbeads was occurring, the microbeads were released into a series of saline solutions of varying osmotic activity. The saline concentrations of the release medium are listed in Table 1 and the total mass fraction released from these experiments is plotted against the release medium osmotic pressure in Figure 7.

In agreement with the proposed osmotic pressure activated release mechanism, the total mass fraction of protein released decreases as the release medium osmotic pressure increases. For example, the mass fraction of LYS released into distilled water was 0.82, and dropped to only 0.15 in a saline solution having an osmotic pressure of 3.17 MPa. The results of Figure 7 also indicate that the osmotic pressure of a saturated LYS solution lies between 2.5 and 3.2 MPa.

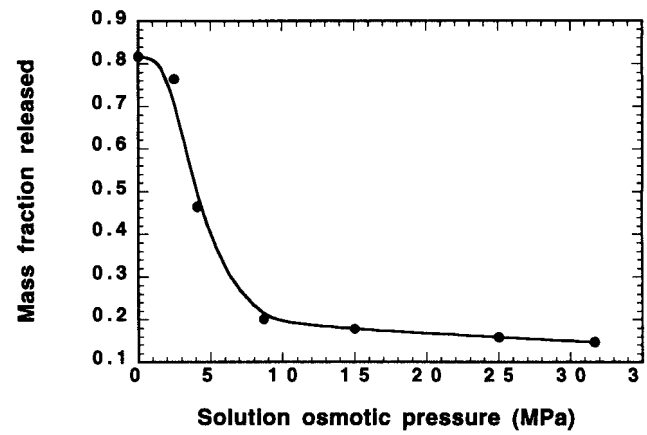

Figure 7. Total mass fraction of lysozyme released from 0.85–0.71 mm microbeads of a volumetric loading of 0.35 and containing < 53 μm particles vs. the osmotic activity of the receiving solution.

Each point represents the average and the error bars represent the standard deviation of three samples.

The osmotic pressure range for this protein at first seemed high when compared to BSA. The saturated solution concentration of BSA has been estimated to be 0.59 g/mL (Saltzman and Langer, 1989), while the saturated solution concentration of LYS was estimated in this study to be about 0.124 g/mL. The osmotic pressure Π of a protein solution can be described by the following expression (Vilker et al., 1981).

$$\Pi = \Re T\left\{2\left[\left(\frac{zC}{2M_w}\right)^2 + m_s^2\right]^{1/2} - 2m_s\right\} + \frac{\Re T}{M_w}(C + A_2C^2 + A_3C^3) \quad (40)$$

in which z is the charge on the protein, C is its concentration, M_w is its molecular weight, m_s is the molar concentration of any salt present, and A_2 and A_3 are virial coefficients which are functions of the charge on the protein. On concentration considerations alone then, the BSA solution should have exhibited a higher osmotic pressure. However, BSA has an isoelectric point of about 4.72 in 0.15 M saline, while the isoelectric point of LYS is 11.0. Since distilled water has a pH of about 6, LYS may carry a more significant charge than does BSA. The larger charge on these proteins could explain the much greater osmotic pressures found for LYS. As well, the protein crystals were used as received and may have contained excess salts. The presence of these salts would also result in a higher osmotic pressure.

The iso-osmotic release experiments were used to find the total mass fraction of particles within the microbeads that were released by diffusion Q_D. Table 2 lists these values for microbeads containing < 53 μm and 106–75 μm LYS particles. The Q_D found for the LYS loaded microbeads agree closely to those obtained for BSA loaded microbeads (Figure 5). In all cases, Q_D increases as the microbead diameter to particle diameter ratio decreases.

The microbeads released into the iso-osmotic saline also displayed a different appearance than those released into distilled water. As prepared, the protein loaded microbeads were generally clear with protein particles protruding from the surface. When immersed in an iso-osmotic saline solution, the appearance of the microbeads did not change. When released into distilled water, however, the microbeads went from clear to milky white in color. This color change normally occurs during polymer fracture (Kaufman and Falcetta, 1977), which would support the proposed osmotic release mechanism. Matrix swelling during agent release by osmotic release mechanisms has been observed by a number of authors for both EVA (Amsden and Cheng, 1994) and silicone (Carelli et al., 1989; Golomb et al., 1990; Schirrer et al., 1992) devices. Although not measured, the microbeads also appeared to swell during release.

Table 2. Diffusional Mass Fraction of Protein Released Q_D from EVA Microbeads Found from Isoosmotic Release Experiments

Particle-Size (μm)	Bead Size (mm)	Q_D
< 53	1.00–0.85	0.12
	0.85–0.71	0.15
	0.71–0.60	0.18
	0.60–0.43	0.20
106–75	1.00–0.85	0.24
	0.85–0.71	0.26
	0.71–0.60	0.29
	0.60–0.43	0.35

More evidence supporting the osmotic release mechanism was obtained from ESEM photomicrographs of LYS loaded microbeads. These pictures were obtained by removing the microbeads from their release media and wiping off excess solution with a tissue. The beads were then placed on a metal support and the pressure reduced slowly to 4–5 torr at room temperature.

Displayed in Figures 8a and 8b are pictures of the surfaces of unreleased microbeads. Clearly present on the undulating surface are LYS particles, along with rather large openings in the surface that are probably due to the process of EVA precipitation. Figure 8c shows the surface of a microbead released into an iso-osmotic saline solution. Again, large openings are present on the surface. Also, there are no LYS particles present on the surface, indicating that the surface particles had dissolved and diffused away. The surfaces of microbeads released into distilled water are shown in Figures 8d and 8e. Not only are there large openings evident and no LYS particles present, but a large number of very small holes can be seen. These "pinholes" are the capsule openings created by the rupturing of the EVA polymer walls.

Osmotic activity of saturated-lysozyme solution

With the presence of the osmotic release mechanism established, the osmotic pressure of a concentrated LYS solution was needed in order to apply the model expression for t_b. As literature values were not available, it was obtained in the following manner. If the radial extension ratio and the tensile strength at rupture of the EVA were known, then the osmotic pressure of a saturated LYS solution could be estimated from the θ values for the microbeads using Eq. 12. The tensile strength of the polymer was found from tensile testing to be 11.1 ± 0.3 MPa, leaving only the radial extension ratio at rupture to be determined.

Since the osmotic activity of a concentrated BSA solution is approximately 0.87 MPa in distilled water, BSA loaded microbeads were used to estimate the radial extension ratio at rupture of the EVA λ_b. The total fraction released from microbeads containing < 53 μm BSA particles of varying size and having a volume fraction loading of BSA of 0.45 was found from release studies done in distilled water. The θ values were then calculated using the Q_D given in Figure 5. These θ values were used to estimate λ_b from a least-squares fit of Eq. 12 to the data. In this fashion λ_b was found to be 2.40 ± 0.04.

The fitted value for λ_b was then used to estimate the osmotic activity of a saturated LYS solution. With osmotic pressure as the manipulated variable, Eq. 12 was fit via a least-squares procedure to the θ data obtained from the LYS release studies (Table 3). The osmotic pressure of a saturated LYS solution was found to be approximately 2.9 ± 0.02 MPa. This value is consistent with the results of Figure 7. In this estimation procedure, it is assumed that the capsule ruptures

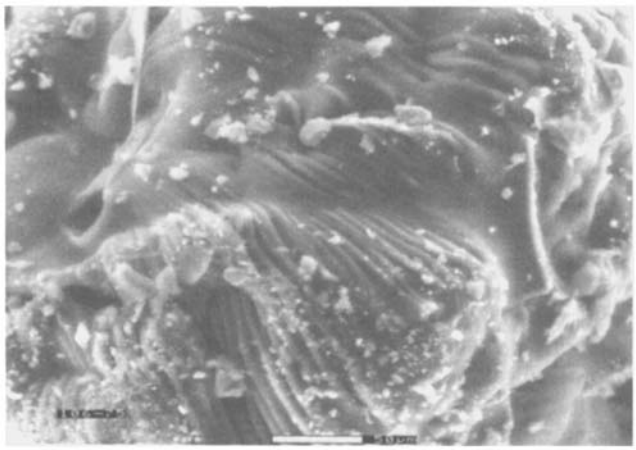

(a)

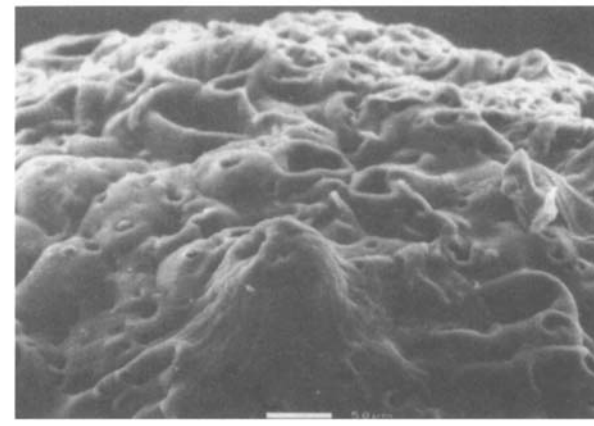

(d)

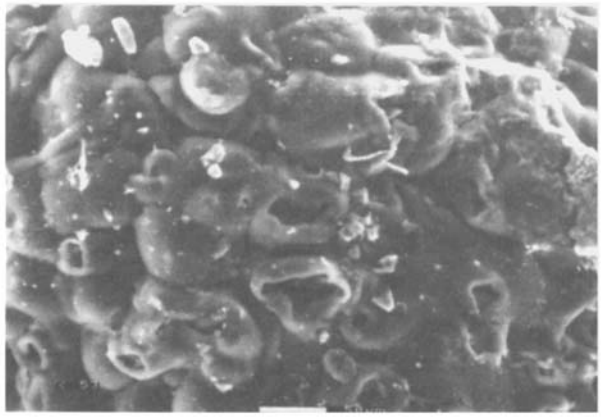

(b)

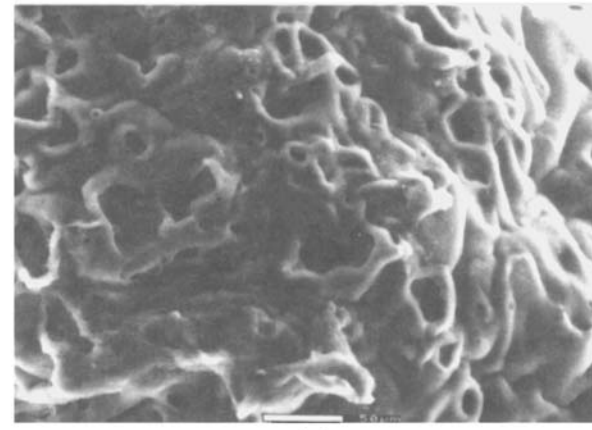

(e)

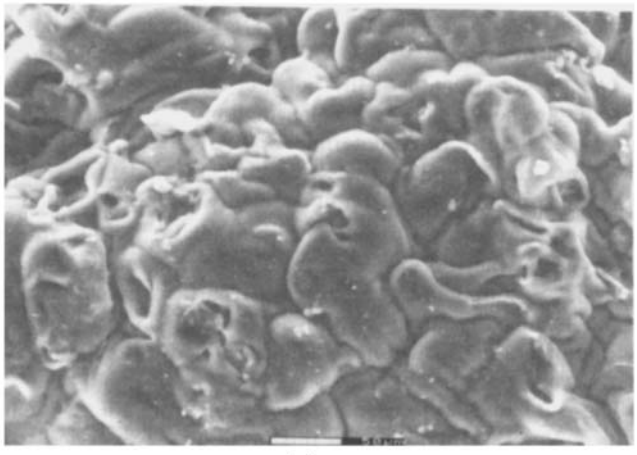

(c)

Figure 8. ESEM images of microbead surface morphology (0.85–0.71-mm microbeads containing < 53 μm particles).

(a) Surface of unreleased microbeads; (b) alternate view of surface of unreleased microbeads; (c) surface of microbead released into iso-osmotic saline; (d) surface of microbead released into distilled water showing numerous "pinholes"; (e)

before all the encapsulated solid dissolves. This work demonstrates a means of estimating the osmotic activity of solutes such as bioactive peptides and proteins that are relatively expensive to work with in large quantities.

Using these Q_D values, the fraction of encapsulated particles released by osmotic bursting θ was calculated and compared to the model predicted values. The values predicted by the model were calculated using an EVA tensile strength at rupture of 11.1 ± 0.3 MPa determined from the uniaxial tensile test. This value of the tensile strength at rupture is in

Table 3. Comparison of Experimentally Determined Osmotic Fraction Released θ to Model Predictions, Based on the Osmotic Pressure at Saturation of BSA Estimated as 0.87 MPa at pH = 6

Protein	Bead Size (mm)	θ Exp.	θ Pred.
BSA ($\phi = 0.45$)	1.00–0.85	0.461	0.453
	0.85–0.71	0.477	0.467
	0.71–0.60	0.502	0.515
	0.60–0.43	0.529	0.531
LYS ($\phi = 0.35$) $< 53\mu$m	1.00–0.85	0.767	0.773
	0.85–0.71	0.785	0.777
	0.71–0.60	0.802	0.785
	0.60–0.43	0.813	0.794
LYS ($\phi = 0.35$) 106–75 μm	1.00–0.85	0.809	0.826
	0.85–0.71	0.837	0.842
	0.71–0.60	0.847	0.858
	0.60–0.43	0.871	0.885

good agreement with the values reported by Salyer and Kenyon (1971). The model predictions agreed quite well to the experimentally determined values, deviating by less than 5% (Table 3). θ increased as the microbead size decreased, and also as the particle size increased, an effect noted previously for a slab geometry (Amsden and Cheng, 1994) and predicted by the model.

Verification of osmotic model

With all the necessary parameters now specified, the model can be applied to the release profiles of the LYS loaded microbeads.

According to the proposed release mechanism, release is initially diffusionally controlled until the osmotic release mechanism starts to dominate. The mass fraction release rate thereby can be written as

$$Q_t = Q_{D,t} + Q_{\Pi,t} \tag{41}$$

in which $Q_{D,t}$ is the mass fraction released at time t. As we are only considering the osmotic release phase, Eq. 41 can be simplified to

$$Q_t = Q_D + Q_{\Pi,t} \tag{42}$$

where Q_D is the total mass fraction released by diffusion. The mass fraction of protein released during the osmotic pressure release phase is given by Eq. 25 which is rewritten below for clarity

$$Q_{\Pi,t} = \frac{\theta(1-Q_D)}{\left[a\left(\frac{R}{x}\right) - \frac{b}{2}\left(\frac{R}{x}\right)^2 + \frac{c}{3}\left(\frac{R}{x}\right)^3\right]} \times \left[a\left(\frac{t}{t_b}\right) - \frac{b}{2}\left(\frac{t}{t_b}\right)^2 + \frac{c}{3}\left(\frac{t}{t_b}\right)^3\right] \tag{25}$$

with t_b given by Eq. 39. The osmotic release mechanism begins as soon as the microbeads are immersed in the release medium with water vapor diffusing through the EVA. Equation 42 was applied only to data above Q_D.

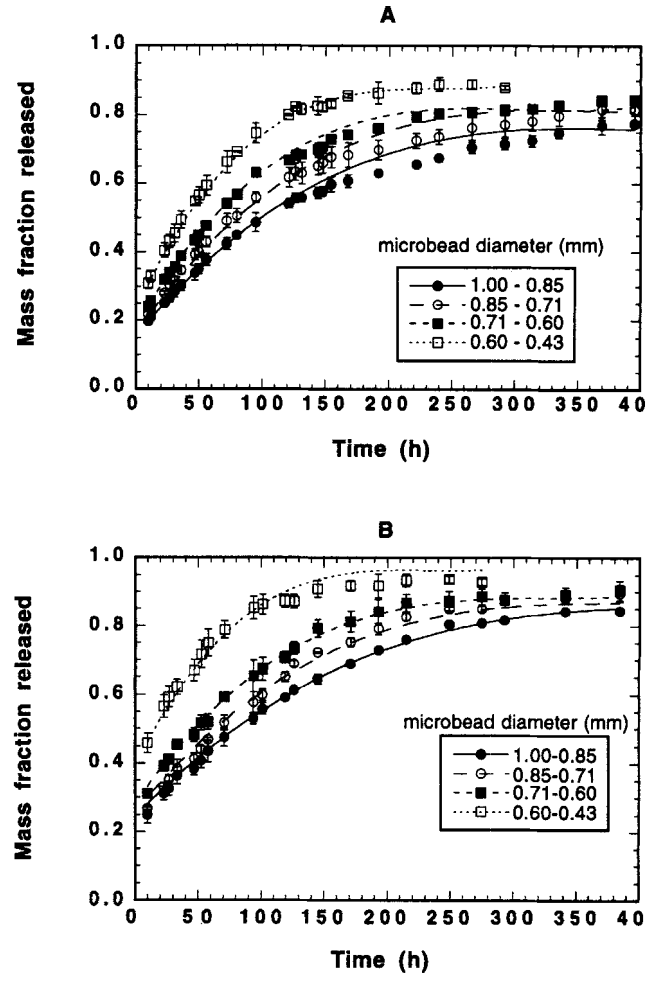

Figure 9. Comparison of model predictions for the osmotic release rate to the experimental data of the osmotic release of lysozyme-loaded microbeads of varying diameter into distilled water.

The lines represent the model predictions. Each point represents the average and the error bars represent the standard deviation of three samples. (a) Microbeads containing < 53 μm particles; (b) microbeads containing 106–75 μm particles.

For the < 53 μm LYS particle loaded microbeads, the value of the time to burst t_b was used directly as predicted by Eq. 39, using $k = 2.1$ (10^{-11}) cm^2/(s·atm) (Amsden et al., 1994). These calculations were done with a Young's modulus value of 7.35 ± 0.25 MPa, determined from the tensile test. This value for the Young's modulus of EVA is in good agreement with the reported values of Salyer and Kenyon (1971). The t_b values for the 106–75 μm LYS loaded microbeads were obtained from a least-squares fit of Eq. 42. The fitted curves are represented as the lines in Figures 9a and 9b. The fitted values obtained for t_b for the 106–75 μm LYS loaded microbeads are listed in Table 4, along with the calculated values using the model equations.

The model provides a very good agreement to the experimental data for the < 53 μm particle containing microbeads

Table 4. Least-Squares Fit of Eq. 42 for $t_{b,\text{fit}}$ to Osmotic Release Phase Data for LYS Loaded Microbeads*

Protein	bsd	$t_{b,\text{fit}}$	$\pm$SE	F_{fit}	$F_{0.05\,df1.df2}$	$t_{b\,\text{calc}}$	$t_{b\,\text{fit}}/t_{b.\text{calc}}$
LYS	1.00–0.85	-	-	1.32	1.92	27.3	1.0
(< 53 μm)	0.85–0.71	-	-	1.34	1.92	27.2	1.0
	0.71–0.60	-	-	1.29	1.98	26.9	1.0
	0.60–0.43	-	-	0.57	1.98	26.6	1.0
LYS	1.00–0.85	103.0	2.9	0.48	2.07	416.0	0.25
(106–75 μm)	0.85–0.71	98.9	1.5	1.47	2.07	404.6	0.24
	0.71–0.60	95.7	4.4	0.57	2.07	392.4	0.24
	0.60–0.43	91.0	1.4	1.45	2.12	371.7	0.25

*Included are the predicted values of t_b.

(Figure 9a), as indicated by a comparison of the fitted F ratio F_{fit} (F_{fit} = estimated variance of the fitted equation/experimentally determined estimate of variance) obtained from the sum of squares of the residuals calculated from the difference between the model predictions and the experimental data at each time point, to tabulated values of the F ratio at the 95% confidence level $F_{0.05,df1,df2}$. This is a promising result since there were no fitted parameters involved in calculating the predicted release behavior. This result also indicates that the assumption that the EVA behaves as a Hookean material is reasonable, at least within the range of material properties of the experiments.

A good agreement between experimental and model predictions could be obtained for the release of LYS from microbeads containing 106–75 μm LYS particles only if the time to burst was considered to be an adjustable parameter in the curve fitting procedure. In this case, the fitted time to burst $t_{b,\text{fit}}$ was 0.24 times smaller than the predicted time to burst $t_{b,\text{calc}}$ (Table 4). The large deviation from model predictions can be explained by examining the assumptions made in the model development.

In developing the time to burst expression, it was assumed that the particles are spherical, that the capsules swelled in a spherical manner, and that the capsule wall thickness was uniform. Neither of these assumptions are likely to be strictly valid. The particles are irregularly shaped, and it has been noted that very high local stresses may be produced within the capsule upon dissolution of irregularly shaped particles (Fedors, 1980). These local stresses may result in capsule swelling which is less in a specific area. Also, larger particles produce larger capsules and the larger the capsule, the greater the tangential stresses at the same osmotic pressure (Schirrer et al., 1992). The presence of these high local stresses would result in the capsule rupturing in a time that is shorter than the predicted time to burst. The time to burst expression, therefore, may be valid only for relatively small particles.

The other model assumptions should also be examined. It was assumed that the particles were of uniform size whereas in fact the particles were sieved into a size range. The diameter distributions of the sieved protein fractions are given in Figures 10a and 10b. The particles are not especially narrowly distributed, which is particularly true for the 106–75 μm LYS particles (Figures 10b). However, the use of an average particle size did not result in a large error in model estimation, as is demonstrated by the close agreement between the model predictions and the experimental data for the fraction of capsules released by rupturing (Table 3). It was also assumed that the particles were distributed homogenously through the matrix. This is a reasonable assumption since the protein-dissolved EVA suspension was well mixed prior to EVA precipitation. The osmotic pressure of the capsule during the water imbibition phase was assumed to be constant. This assumption is not strictly valid as it will take a certain period of time for the solution to reach saturation. However, for readily soluble agents such as LYS, this period

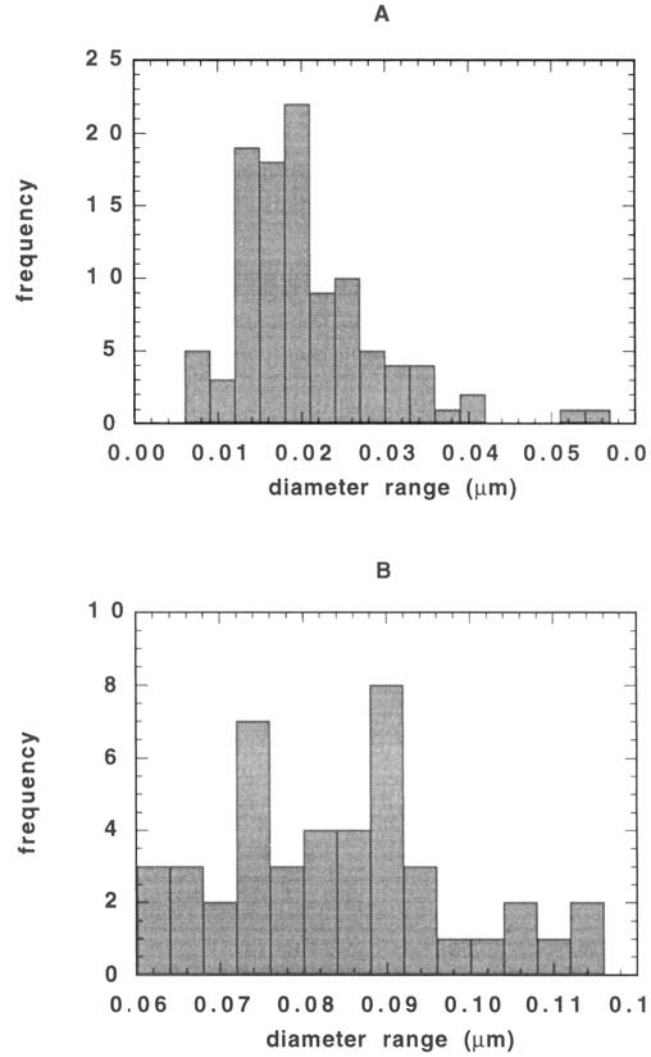

Figure 10. LYS particle-size distributions.

(a) < 53 μm LYS particles; (b) 106–75 μm LYS particles.

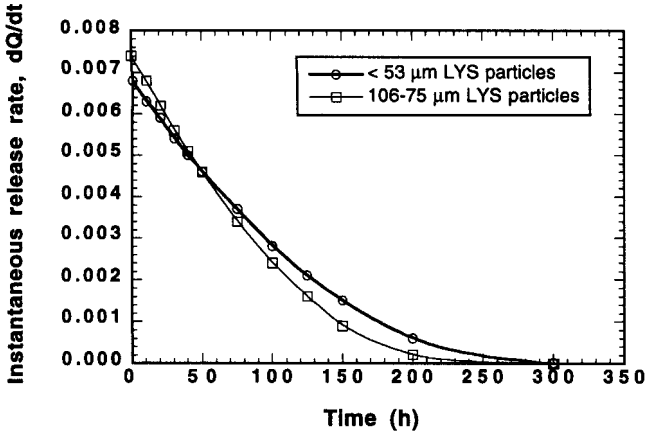

Figure 11. A comparison of the calculated instantaneous release rates of 0.60–0.43 mm LYS-loaded microbeads containing < 53 μm particles and 106–75 μm particles.

of time would likely be negligible when compared to the total time required to rupture the capsule. Thus, the assumption is reasonable.

Finally, the effect of particle size on the release rate should be examined. According to the model developed in this article, larger particles incorporated at the same volumetric loading as smaller particles require a longer time to rupture (Table 4), which would lead to a slower release rate. However, when the larger capsules rupture they release a greater quantity of agent. The effect of particle size on the release rate therefore requires a close examination of the defining release rate equation.

From Eq. 25 the osmotic release rate from a microbead is given by

$$\frac{dQ_{\Pi,t}}{dt} = \frac{\theta(1-Q_D)}{\left[a\left(\frac{R}{x}\right) - \frac{b}{2}\left(\frac{R}{x}\right)^2 + \frac{c}{3}\left(\frac{R}{x}\right)^3\right] t_b} \times \left[a - b\left(\frac{t}{t_b}\right) + c\left(\frac{t}{t_b}\right)^2\right] \quad (43)$$

Equation 43 was used to compare the release rates of LYS loaded microbeads of an average diameter of 0.25 mm and containing < 53 and 106–75 μm particles. The value of t_b used for the < 53 μm case was that calculated using Eq. 37, whereas the value of t_b used for the 106–75 μm case was that obtained from the curve fitting procedure. The results are displayed in Figure 11.

The release rate is a function of time and is initially larger for the microbeads containing the larger particles (Figure 11). As time progresses, the release rate for the microbeads containing the larger particles decreases more rapidly than does the release rate for microbeads containing the smaller particles. At some point, approximately 50 h for the microbeads considered here, the release rate for the smaller microbeads becomes greater. This crossover effect is a result of the geometry of the release device and the difference in the time required to burst a capsule. There is a greater amount of agent released in the initial layers of the microbeads containing the larger particles, but the amount released decreases more rapidly as the release front approaches the center of the bead than it does for the smaller microbeads. This change in the amount of agent, coupled with the fact that the smaller capsules rupture about three times faster, results in the release rate from the microbeads containing smaller particles becoming greater than that for microbeads containing larger particles. However, as indicated in Figure 11, the release rates are not dramatically different at any time.

Conclusions

The release of an agent from a spherical polymer microbead matrix can be significantly affected by its osmotic activity. The osmotic pressure generated by the encapsulated agent particles results in an increased mass fraction being released, and a prolonged release duration. The mass fraction released increases as the particle size increases and as the microbead size decreases. Osmotic release rates were found to increase as the microbead radius increases, and were only a weak function of the agent particle size.

A mechanistic model was developed which was consistent with the observed results. The model can be used in the design and development of controlled release devices for pharmaceutical, veterinarial, and agricultural applications. Another interesting application of the model is to estimate the osmotic activity of a given agent at saturation once the pertinent polymer properties are known. These properties can be determined from release studies of an agent whose osmotic activity is known.

Acknowledgments

This work was partly funded by the Ontario Centre for Materials Research. The author would like to thank DuPont Canada for donating the EVA, Dr. T. Harris and Dr. T. Grandmaison, Dept. of Chemical Engineering, Queen's University, for their help in preparing the manuscript, and Paul Nolan of the Dept. of Materials and Metallurgical Engineering, Queen's University for the ESEM pictures.

Notation

$df1$ = degrees of freedom associated with the fitted estimate of variance

$df2$ = degrees of freedom associated with the experimentally determined estimate of variance

Literature Cited

Amsden, B. C., "Microbead Embedded Hydrogel as Drug Reservoir for Transdermal Macromolecular Drug Delivery," PhD Thesis, Queen's Univ. (1996).

Amsden, B. G., and M. Goosen, "An Examination of Factors Affecting the Size, Distribution, and Release Characteristics of Polymer Microbeads Made Using Electrostatics," *J. Contr. Rel.*, accepted (1996).

Amsden, B. G., and Y.-L. Cheng, "A Generic Peptide Delivery System Based on Osmotically Rupturable Monoliths," *J. Contr. Rel.*, **33**, 99 (1995).

Amsden, B. G., Y.-L. Cheng, and M. F. A. Goosen, "A Mechanistic Study of the Release of Osmotic Agents from Polymeric Monoliths," *J. Contr. Rel.*, **30**, 45 (1994).

Amsden, B. G., and Y.-L. Cheng, "Enhanced Fraction Releasable Above Percolation Threshold from Monoliths Containing Osmotic Excipients," *J. Contr. Rel.*, **31**, 21 (1994).

Baker, R., *Controlled Release of Biologically Active Agents*, Wiley, Toronto (1987).
Bugarski, B., B. Amsden, R. J. Neufeld, D. Poncelet, and M. F. A. Goosen, "Effect of Electrode Geometry and Charge on the Production of Polymer Microbeads by Electrostatics," *Can. J. Chem. Eng.*, **72,** 517 (1994).
Bugarski, B., Q. Li, M. F. A. Goosen, D. Poncelet, R. J. Neufeld, and G. Vunjak, "Electrostatic Droplet Generation: Mechanism of Polymer Droplet Formation," *AIChE J.*, **40,** 1026 (1994).
Carelli, V., G. Di Colo, C. Guerinni, and E. Nannpieri, "Drug Release From Silicone Elastomers Through Controlled Polymer Cracking: An Extension To Macromolecular Drugs," *Int. J. Pharm.*, **50,** 181 (1989).
Di Colo, G., V. Campigli, V. Carelli, E. Nannipieri, M. F. Serafini, and D. Vitale, "Release of Osmotically Active Drugs from Silicone Rubber Matrices," *Il Farmaco, Ed. Pr.*, **39,** 310 (1984).
Fedors, R. F., "Osmotic Effects in Water Absorption by Polymers," *Polymer*, **21,** 207 (1980).
Fossey, D. J., and C. H. Smith, "The Fabrication of Open-Cell Polyethylene Foam," *J. Cellular Plast.*, **9**, 268 (1973).
Gale, R., S. K. Chandrasekaran, D. Swanson, and J. Wright, "Use of Osmotically Active Therapeutic Agents in Monolithic Systems," *J. Memb. Sci.*, **7**, 319 (1980).
G. Golomb, P. Fisher, and E. Rahamim, "The Relationship Between Drug Release Rate, Particle Size and Swelling of Silicone Matrices," *J. Contr. Rel.*, **12,** 121 (1990).
Kaufman, H. S., and J. J. Falcetta, *Introduction to Polymer Science and Technology: An SPE Textbook*, Wiley, Toronto (1977).
Kuethe, D. O., D. C. Augenstein, J. D. Gresser, and D. L. Wise, "Design of Capsules that Burst at Predetermined Times by Dialysis," *J. Contr. Rel.*, **18,** 159 (1992).
Marson, F., "Antifouling Paints I. Theoretical Approach to Leaching of Soluble Pigments from Insoluble Paint Binders," *J. Appl. Chem.*, **19,** 93 (1969).
McGinity, J. W., L. A. Hunke, and A. B. Combs, "Effect of Water-Soluble Carriers on Morphine Sulfate Release From a Silicone Polymer," *J. Pharm. Sci.*, **68,** 662 (1979).
Narkis, N., and M. Narkis, "Slow Release of Water-Soluble Salts from Polymers," *J. Appl. Polym. Sci.*, **20,** 3431 (1976).
Robinson, R., and R. Stokes, *Electrolyte Solutions*, 2nd ed., Butterworth Publications, London (1965).
Saltzman, W., and R. Langer, "Transport Rates of Proteins in Porous Materials with Known Microgeometry," *J. Biophys.*, **55,** 163 (1989).
Salyer, I. O., and A. S. Kenyon, "Structure and Property Relationships in Ethylene-Vinyl Acetate Copolymers," *J. Polym. Sci. Part A-1,9*, 3083 (1971).
Scatchard, G., A. C. Batchelder, A. Brown, and M. Zosa, "Preparation and Properties of Serum and Plasma Proteins. VII. Osmotic Equilibria in Concentrated Solutions of Serum Albumin," *J. Amer. Chem. Soc.*, **68,** 2610 (1946).
Schirrer, R., P. Thepin, and G. Torres, "Water Absorption, Swelling, Rupture, and Salt Release in Salt-Silicone Rubber Compounds," *J. Mat. Sci.*, **27,** 3424 (1992).
Sefton, M. V., L. Brown, and R. Langer, "Ethylene-Vinyl Acetate Microspheres For Controlled Release Of Macromolecules," *Pharm. Sci.*, **73**, 1859 (1984).
Siegel, R. A., J. Kost, and R. Langer, "Mechanistic Studies of Macromolecular Drug Release from Macroporous Polymers I. Experiments and Preliminary Theory Concerning Completeness of Drug Release," *J. Contr. Rel.*, **8**, 223 (1989).
Vilker, V. L., C. K. Colton, and K. A. Smith, "The Osmotic Pressure of Concentrated Protein Solutions: Effect of Concentration and pH in Saline Solutions of Bovine Serum Albumin," *J. Coll. Interface Sci.*, **79,** 548 (1981).
Wright, J., S. K. Chandrasekaran, R. Gale, and D. Swanson, "A Model for the Release of Osmotically Active Agents from Monolithic Polymeric Matrices," *AIChE J.*, **27**(206), 62 (1981).
Zhang, X., U. P. Wyss, D. Pichora, B. Amsden, and M. F. A. Goosen, "Controlled Release of Albumin From Biodegradable Poly(DL-Lactide) Cylinders," *J. Contr. Rel.*, **25,** 61 (1993).

Manuscript received Nov. 15, 1995, and revision received Apr. 24, 1996.